HHS Public Access

Author manuscript

Biochemistry. Author manuscript; available in PMC 2016 April 21.

Published in final edited form as:

Biochemistry. 2015 April 21; 54(15): 2530–2538. doi:10.1021/acs.biochem.5b00135.

Mechanistic Studies of Inactivation of Inducible Nitric Oxide Synthase by Amidines

Wei Tang[1], **Huiying Li**[2], **Thomas L. Poulos**[*,2], and **Richard B. Silverman**[*,1]

[1]Department of Chemistry, Department of Molecular Biosciences, Chemistry of Life Processes Institute, and Center for Molecular Innovation and Drug Discovery, Northwestern University, 2145 Sheridan Road, Evanston, Illinois 60208-3113, United States

[2]Department of Molecular Biology and Biochemistry, Chemistry, and Pharmaceutical Sciences, University of California, Irvine, California 92697-3900, United States

Abstract

Nitric oxide synthase (NOS) catalyzes the conversion of L-arginine to L-citrulline and nitric oxide. N^5-(1-Iminoethyl)-L-ornithine (L-NIO), an amidine-containing molecule, is a natural product known to be an inactivator of inducible NOS (iNOS). Because of the presence of the amidine methyl group in place of the guanidine amino group of substrate L-arginine, the active site heme peroxy intermediate sometimes cannot be protonated, thereby preventing its conversion to the heme oxo intermediate; instead, a heme oxygenase type mechanism occurs, leading to conversion of the heme to biliverdin. This might be a new and general inactivation mechanism for heme-containing enzymes. In the studies described here, we attempted to provide support for amidines as substrates and inactivators of iNOS by the design and synthesis of amidine analogues of L-NIO having groups other than the amidine methyl group. No nitric oxide or enzyme-catalyzed products could be detected by incubation of these amidines with iNOS. Although none of the L-NIO analogues acted as substrates, they all inhibited iNOS; increased inhibitory potency correlated with decreased substituent size. Computer modeling and molecular dynamics simulations were run on **10** and **11** to rationalize why these compounds do not act as substrates. Unlike the methyl amidine (L-NIO), the other alkyl groups block O_2 binding at the heme iron. Compounds **8**, **9**, and **11** were inactivators, but no heme was lost and no biliverdin was formed. No kinetic isotope effect on inactivation was observed with perdeuterated ethyl **8**. A small amount of dimer disruption occurred by these inactivators, although the amount would not account for complete enzyme inactivation. The L-NIO analogues inactivate iNOS by a yet unknown mechanism, but it is different from that of L-NIO, and the inactivation mechanism previously reported for L-NIO appears to be unique to methyl amidines.

[*]Corresponding authors: Professor Richard B. Silverman: Tel.: +1 847 491 5653; rsilverman@northwestern.edu. Professor Thomas L. Poulos: Tel.: +1 949 824 7020; poulos@uci.edu.

Supporting Information

Kinetic data for **8, 9, 11,** and **26**, HPLC of control, **4, 8, 9,** and **11** with iNOS, preparation and characterization of compounds, and ^{1}H NMR and ^{13}C NMR spectra of inhibitors. This material is available free of charge via the Internet at http://pubs.acs.org.

Notes

The authors declare no competing financial interest.

Nitric oxide (NO) is an important cell-signaling agent, which is synthesized *in vivo* from oxygen and L-arginine by the enzyme called nitric oxide synthase (NOS, EC 1.14.13.39).[1] The importance of understanding the chemistry and biochemistry of NO has been highlighted in fields as diverse as immunology and reproductive technology, while the inhibition of NO biosynthesis has been an important approach for the design of drugs to treat septic shock, rheumatoid arthritis, stroke, Alzheimer's disease, and Parkinson's disease.[2, 3, 4, 5] There are three mammalian NOS isoforms: neuronal nitric oxide synthase (nNOS), endothelial nitric oxide synthase (eNOS), and inducible nitric oxide synthase (iNOS), which exhibit 50-60% sequence identity and share identical overall architecture.[6, 7]. The active sites of NOS isozymes are highly conserved; 16 of 18 residues within 6 Å of the substrate binding site of nNOS and eNOS are identical, and the side chain of one of the two dissimilar amino acids points out of the substrate-binding site.[8] Therefore, there is only a one amino acid difference to take advantage of in the active sites of these two isoforms.

However, since NOS inhibition may also be detrimental to the essential functions of NO, selective inhibition of individual NOS isoforms is important for the development of therapeutics.

In the presence of O_2, NOS converts L-arginine (**1**) to L-citrulline (**3**) and NO with concomitant oxidation of nicotinamide adenine dinucleotide phosphate hydrogen (NADPH) (Scheme 1). Numerous cofactors bind to NOS, including flavin mononucleotide (FMN), flavin adenine dinucleotide (FAD), NADPH, protoporphyrin IX, and tetrahydrobioperin (H_4B). Each NOS isoform is calmodulin (CaM) dependent, although iNOS has been shown to bind CaM very tightly regardless of change in cellular Ca^{2+} levels;[9] therefore, iNOS is kinetically independent of Ca^{2+} concentration. NOS is active only as a homodimer,[10] with each monomer consisting of two subdomains. Inspection of the peptide sequence of NOS and the crystal structure of iNOS[11] reveals a C-terminal and an N-terminal domain. Sequences in the C-terminal domain of NOS contain binding sites for FMN, FAD, and NADPH.[12] The C-terminal domain serves to shuttle electrons from the two-electron donor, NADPH, through the one or two electron acceptor/donors, FMN and FAD, to the H_4B[13,14] and heme cofactors in the N-terminal domain of the other monomer.[15] The H_4B is believed to be involved in electron donation to the heme, [16, 17, 18] where substrate oxidation occurs; [19, 20] during the catalytic cycle the oxidized H_4B becomes rereduced.[21,22] Calmodulin and Ca^{2+} are required to enable the electron transfer between the domains.[23,24]

Fast et al.[25] reported that the natural product N^5-(1-iminoethyl)-L-ornithine (L-NIO) (**4**) is a time-, concentration-, and NADPH-dependent iNOS inactivator, and it acted as a substrate as well as an inactivator of iNOS. Incubation of iNOS with L-NIO leads to loss of the heme cofactor from the enzyme and the formation of biliverdin, as monitored by HPLC and LC/MS analysis. The same conversion of heme cofactor to biliverdin was identified by Zhu et al.[26] from the inactivation of iNOS by *N*-(3-(aminomethyl)benzyl)acetamidine (1400W) (**5**). It was proposed that L-NIO, 1400W, and possibly all amidine-containing

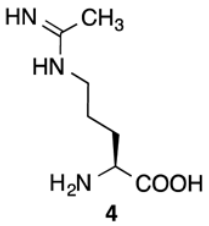

4

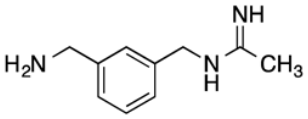

5

inactivators of NOS, inactivate the enzyme by preventing protonation of the heme peroxide intermediate, which is believed to occur by the guanidinium group of L-arginine, thereby preventing the formation of the heme iron-oxo species and the normal substrate oxygenation (Scheme 2). Instead, a self-oxidation and irreversible inactivation of NOS occurs with conversion of its heme cofactor into biliverdin, along with the production of carbon monoxide (Scheme 3). This is a unique example of inactivation of an enzyme, because the inactivator is not modified during inactivation phase. On the basis of the results that L-NIO acts both as a substrate and inactivator, we hypothesized that L-NIO might bind with either the CH_3 or the NH^{2+} adjacent to the catalytic heme; when the NH^{2+} group is rotated over the heme, oxygenation to N-hydroxy-L-arginine occurs (**2**, Scheme 1), but when the methyl group is rotated toward the heme, inactivation occurs (Scheme 3). This is a reasonable hypothesis because interchange of the CH_3 and the NH_2^+ groups in L-NIO would not cause any steric problems in the NOS active site. However, it is known that N^{ω}, $N^{\omega\omega}$-dimethylarginine (**6a**) is an endogenous NOS inhibitor, but N^{ω},N'^{ω}-dimethylarginine (**6b**) is inactive,[27] indicating that the binding of **6b** is intolerable in the NOS pocket which is too

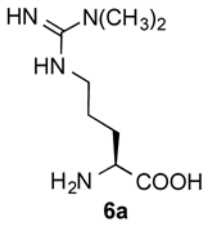

6a

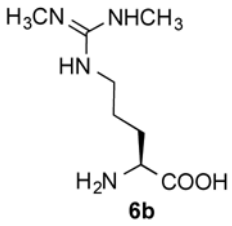

6b

narrow to allow the methyl group on both terminal guanidine nitrogens. We, therefore, designed and synthesized analogues of L-NIO with variable groups (R) at the terminus (Figure 1 to determine whether rotation of the amidine bond is indeed affected by R group size, and if it determines substrate turnover compared with inactivation. The results of these studies are described here.

EXPERIMENTAL PROCEDURES

General methods

All syntheses were conducted under anhydrous conditions in an atmosphere of argon, using flame-dried apparatus and employing standard techniques in handling air-sensitive materials. Non-synthesized reagents were purchased from Sigma – Aldrich Co. and TCI, and were used without further purification. Propanenitrile-d_5 was purchased from CDN Isotopes. ^{1}H NMR spectra were recorded on 500 MHz Varian or Bruker AVANCE spectrometers. Data are presented as follows: chemical shift (in ppm on the δscale relative to δ = 0.00 ppm for the protons in TMS), integration, multiplicity (s = singlet, d = doublet, t =

triplet, q = quartet, m = multiplet), coupling constant (J/Hz). Coupling constants were taken directly from the spectra and are uncorrected. ^{13}C NMR spectra were recorded at 125 MHz, and all chemical shift values are reported in ppm on the δ scale. All ion exchange chromatography was performed using Dowex 50WX8-200 resin. Chemical shifts are reported as δ values in parts per million with the $CDCl_3$, D_2O, and CD_3OD peaks set at 7.26, 4.80, and 3.31 ppm, respectively. An Orion research model 701H pH meter with a general combination electrode was used for pH measurements. LC–MS (ESI) was conducted on an Agilent MSD mass spectrometer. High-resolution mass spectra (HRMS) were measured with an Agilent 6210 LC-TOF (ESI) mass spectrometer. Optical rotations were measured on a PerkinElmer Model 341 digital readout polarimeter. The enzyme assay was monitored on a BioTek Synergy 4 microplate reader. A Beckman System Gold 125P solvent module was used to run HPLC.

Enzyme Expression and Purification

The expression and purification of recombinant murine iNOS from *Escherichia coli* was performed according to the methods reported by Stuehr and Ikeda-Saito.[28]

Hemoglobin Assay for iNOS Activity

The production of NO was measured by the rapid oxidation of oxyHb to metHb by nitric oxide.[28] The assay mixture contained L-arginine (10 μM), NADPH (100 μM), oxyhemoglobin (0.125 mg/mL), tetrahydrobiopterin (10 μM), and different amounts of inhibitors. The final volume was adjusted to 600 μL with 100 mM Hepes buffer, pH 7.4. The enzymatic reaction was initiated by addition of 10 μL of iNOS stock, and the rate of NO production was monitored by the change in absorbance at 401 nm in the initial 60 s on a spectrophotometer at 37 °C. Curves were fit using the Michaelis– Menten equation in GraphPad Prism 5.0 (GraphPad Software, Inc.). For *K*i determinations, IC_{50} values were calculated using nonlinear regressions (dose-response inhibition, four-parameter variable slope). Subsequent *K*i values were calculated using the Cheng-Prusoff relationship: $K_i = IC_{50}/(1 + [S]/K_m)$ (K_m for murine iNOS is 8.3 μM).[29]

HPLC of Amino Acid Metabolites

The inactivation mixture was derivatized with *o*-phthalaldehyde and 2-mercaptoethanol. Inactivation mixtures contained 11.2 μL of **4, 7**-**13** (2 mM), 6.7 μL of Hepes buffer (100 mM, pH 7.4), 3.3 μL of catalase (3.42 mg/249 μL), 13.8 μL glycerol, 32 μL NADPH (39 mM), 15.7 μL H_4B (8 mM), and 64 μL of iNOS stock. The mixture was incubated at 37 °C for 3 h until completion of inactivation. Aliquots (10 μL) were removed and added to 20 μL of *o*-phthalaldehyde /2-mercaptoethanol (20:1, v/v) reagent. The sample was injected onto an Econosil C_{18} HPLC column (Alltech, 10 μm, 250 mm × 4.6 mm). A Beckman System Gold 125P solvent module was used to control the gradient elution as follows: Isocratic elution with 90% solvent A: 10% solvent B was carried out for 5 min. The contents of solvent B were then increased linearly to 100% over a period of 10 min. 100% solvent B was carried out for 10 min. Solvent A was 50 mM sodium acetate, pH 5.9. Solvent B was 80% (v/v) methanol and 20% (v/v) solvent A. Sample elution was detected by absorbance at 340 nm with a flow rate of 1.0 mL/min.

Irreversible Inhibition Kinetics

The same inactivation mixtures were prepared as noted in HPLC of Amino Acid Metabolites section. The reactions were initiated by the addition of enzyme, and 10 μL aliquots were removed at specified time points and tested via the initial velocity assay. Controls were performed by replacing the inhibitor solution with Hepes buffer. K_I and k_{inact} values were determined by the method of Kitz and Wilson.[30]

Activity Recovery Determination

The incubation mixture for enzyme activity recovery determination contains 70 μM of potential inactivator. When the incubation mixture showed an obvious activity loss after 16 h at 0 °C, microdialysis was performed over 16 h. The total incubation volume was 100 μL, which was dialyzed in a volume of 100 mL Hepes buffer, pH 7.4. The Hepes buffer was changed two times, every 5 h. All of the incubation mixtures with different compounds and the control were distributed into separate flasks to avoid any cross-contamination. The enzyme activity recovery was checked after overnight dialysis.

HPLC and LC/MS Determination of Biliverdin

Biliverdin determination after treatment of iNOS with **4, 7**-**13** was carried out by LC/MS with diode array detection, using a C_{18} reversed-phase column (Vydac, 218TP54, 5 μm, 4.6 × 250 mm) at 401 nm with 60% H_2O (0.1% TFA) and 40% CH_3CN (0.1% TFA) at a flow rate of 1.0 mL/min. Injections were made after the incubation mixture containing compounds **4**, **8**, **9**, or **11** no longer showed iNOS activity. A gradient method was used: solvent B began at 40% and was then increased linearly to 60% over a period of 10 min. 60% solvent B was decreased to 40% B in 2 min and 40% B was carried out for 3 min.

Computer Modeling of 10 and 11 in iNOS

Models of **10** and **11** were manually built according to the binding model of substrate (L-Arg) and docked to the murine iNOS structure (IN2N). Crystallographic waters were retained, and the system was further solvated in an octahedral unit cell with a 10 Å cushion. Sodium ions were added to maintain net neutrality giving a total of 75,195 and 75,201 atoms for the **10** and **11** complex, respectively. The Amber 12.0 suite (http://ambermd.org/) was used for all calculations.[31] The ff10 force field provided with the Amber 12.0 package was used for the protein, while the heme-Cys ligand parameters were taken from Shahrokh et al.[32] Parameters for **10** and **11** were derived with antechamber and the gaff force field[33] using the BCC charging scheme.[34,35]

The structure was prepared for production molecular dynamics runs by first energy minimization for 1000 cycles with all heavy atoms except water molecules fixed in position followed by another 1000 cycles where only the inhibitor atoms were allowed to move. In the final 1000 cycles all atoms were allowed to move. Production runs were carried out with a 1 fs time step and coordinates saved every 10 ps. Temperature and pressure were held constant through weak coupling with a 1 ps pressure relaxation time and Langevin dynamics using a collision frequency of 1 ps^{-1}. Periodic boundary conditions were used with a Particle Mesh Ewald implementation of the Ewald sum for the description of long-range

electrostatic interactions.[36] A spherical cutoff of 10.0 Å was used for nonbonded interactions. Bonds involving hydrogen atoms were constrained using SETTLE.[37] Analysis was carried out using the Amber software suite.

RESULTS

Syntheses of 4, 7-13, 22, and 26

Compounds **4, 7-13** (Figure 1) were synthesized as shown in Scheme 4. The synthesis of all of the L-NIO analogues started by alcoholysis of nitriles **14**, converting them to the corresponding imidic esters (**15**).[25,38,39] Boc-protected L-NIO analogues (**16**) were produced by condensation of Boc-L-Orn-OH and **15**. After removal of the Boc group by treatment with 4 M aqueous HCl, compounds **4, 7-13** were obtained.

The reactions producing **10-12** did not proceed to completion, despite extended reaction times, and the unreacted Boc-L-Orn-OH was difficult to remove by chromatography. Therefore, to remove **17** the reaction mixture was subjected to *N*-(3-dimethylaminopropyl)-*N*′-ethylcarbodiimide (EDC) lactamization (Scheme 5),[40] to form lactam **18**, which was easily removed by extraction.

Compound **22**, the potential hydroxylation metabolite of **8**, was synthesized as shown in Scheme 6; oxime **20** was made from propanal (**19**).[41] Compound **22** was obtained after removal of the Boc protecting group.

Compound **26** was successfully prepared following the synthetic route below (Scheme 7). Starting with propanenitrile-d_5 (**23**), a Pinner reaction was used to make imidic ester **24**. Substitution with Boc-L-Orn-OH gave **25**, and the Boc group was removed in 4 M HCl to give **26**.

Determination of Substrate Activity, Inhibition Constants (IC_{50}), and Inhibition Type

None of the L-NIO analogues generated any NO at concentrations up to 2 mM. Inhibition experiments were performed by measuring the velocity of NO generation after using different concentrations of the inhibitor and different concentrations of substrate L-arginine. Inhibition of iNOS decreased as the alkyl group became more bulky (Table 1). The only exception is the reversal of K_i values for **10** and **11**. L-NIO and all analogues except **12** were found to be competitive inhibitors; **12** was a noncompetitive inhibitor.

Inactivation of iNOS by 8, 9, and 11

Compounds **8**, **9,** and **11** (Figure 1) were inactivators of iNOS, and their dissociation constants were measured. [43] Inactivation experiments were performed by measuring the enzyme activity remaining after incubation with different concentrations of the inactivator with the cofactors and iNOS. As shown in Table 2, L-NIO (**4**) is a more efficient inactivator than **8**, **9**, and **11**, although the inactivation rate constants (k_{inact}) for **8**, **9**, and **11** are greater than that for **4**.

Metabolites from Inactivation of iNOS by 8, 9, and 11

HPLC analysis of the amino acid metabolites from **8**, **9**, and **11** inactivation using *o*-phthaldialdehyde (OPA) and 2-mercaptoethanol (MCE) was conducted.[25, 44, 45] LC/MS was employed to characterize any metabolites formed; however, none was detected. Compound **22** was synthesized as a standard for the potential *N*-hydroxylated metabolite of **8**; no **22** was observed.

Kinetic Isotope Effect on Inactivation of iNOS by 8 and 26

Inactivation of iNOS with (*S*)-2-amino-5-(propanimidamido-2,2,3,3,3-d_5)pentanoic acid (**26**) showed no kinetic isotope effect on ${}^{H}k_{inact}/{}^{D}k_{inact}$ (1.025 (±0.071)) or on ${}^{H}(k_{inact}/K_I)/{}^{D}(k_{inact}/K_I)$ (1.159 (±0.108)) (Table 3).

Detection of Heme and Biliverdin from Inactivation of iNOS by 8, 9 and 11

L-NIO and 1400W both convert the active site heme in iNOS to biliverdin IXα, determined by LC-electrospray mass spectrometry and by HPLC analysis.[26] No apparent heme loss or biliverdin formation was observed from incubation of iNOS with **8**, **9,** or **11**.

LT-PAGE Assay

To determine whether **8**, **9**, and **11** inactivate iNOS by disruption of the homodimer structure to monomers, iNOS was incubated with L-NIO (**4**), **8**, **9**, and **11**, and low temperature SDS-polyacrylamide gel electrophoresis (LT-PAGE) was performed. The gels were stained with SYPRO tangerine protein gel stain and imaged for protein quantitation in a Typhoon 9400 imager with a blue laser beam at 488 nm wavelength. It was reported that the addition of 1 μM L-Arg and 0.2 mM H_4B produced a stable and noncovalently linked iNOS dimer;[46] both the iNOS monomer and dimer were present on the gel. Less dimer was detected after incubation with L-NIO (**4**), **8**, **9**, and **11** (Figure 2). The amounts of dimer and monomer remaining after inactivation are shown in Table 4.

DISCUSSION

On the basis of no nitric oxide having been produced and no products detected by LC/MS from incubation of iNOS with up to 2 mM **7**-**13**, it can be concluded that these compounds do not act as substrates, unlike L-NIO (**4**).

Compounds **7**-**13** all inhibited iNOS activity; all are competitive reversible inhibitors except **12**, which is a noncompetitive reversible inhibitor, and **8**, **9**, and **11**, which are irreversible inhibitors. The inhibitor potency decreases as the amidine alkyl group becomes larger; **7**, which has the smallest sized R group (H), was the most potent inhibitor of iNOS, with a K_i = 0.18 μM. This implies that the active site pocket of iNOS has sufficient room to fit a bulky group at the amidine terminus, but the larger the substituent, the greater the steric hindrance with surrounding residues. The only reversal in apparent size is **10** and **11**, with the K_i for the isobutyl analogue (**11**) being half of that for the isopropyl analogue (**10**).

Since crystal structures of these L-NIO analogues bound to iNOS were not available, computer models of **10** and **11** were manually built according to the binding model of

substrate (L-Arg) and docked into the murine iNOS structure (IN2N).[47] The docked models were then energy minimized and subjected to molecular dynamic simulations. The models right after the initial minimization are shown in Figure 3 and those of the final frame of the simulation in Figure 4. Both **10** and **11** remain stably bound throughout the 1 ns MD simulation. The side chain isopropyl and isobutyl groups of **10** and **11**, respectively, are tucked into a hydrophobic pocket lined by Pro344, Val346, and Phe363.

In the computer model of **10** after minimization (Figure 3A), tight contacts are shown between the isopropyl group and the Pro344 carbonyl as well as the heme iron, whereas **11** does not have those tight contacts (Figure 3B). MD calculations relax all of the tight contacts but at the cost of distortion of the ligand's geometry, especially around the amino acid moiety, which departs from what is known about how L-Arg binds (Figure 4). Although just computer models, it is interesting that after minimization they are more agreeable with the K_i measurements, where **10** has poorer binding affinity than **11**. This may result from steric crowding of **10**; **11** has a longer, and therefore more flexible, isobutyl tail, which can avoid unfavorable steric clashes and instead make more favorable nonbonded contacts (Figure 3).

Over the course of the simulation the distance between the center of mass of the alkyl groups and iron is 4.49 ± 0.30 Å and 3.90 ± 0.17 Å for **10** and **11**, respectively, with the alkyl groups remaining positioned directly over the iron. The low standard deviation indicates that the alkyl groups are quite stable and remain close to the heme iron. Such a close approach directly over the iron leaves insufficient room for O_2 to bind, which would preclude their substrate activity, as observed. In sharp contrast, L-NIO is isosteric with L-Arg, and the crystal structure of the eNOS-L-NIO complex (a structure in iNOS is not available)[48] shows that there is sufficient room for O_2 to bind to the heme iron. Moreover, the comparable size of NH_2 and CH_3 of the acetamidino of L-NIO allows either the protonated imino group to be available to donate a proton to the heme peroxide and act as a substrate or the methyl group to block proton donation and lead to inactivation, as observed. In contrast, the L-NIO analogues with larger alkyl group cannot rotate, because of the limited space in the NOS active site (Figure 3), to bring the imino group closer to the iron. Therefore, blockage of O_2 binding to heme and the lack of a close proton donor are the reasons why compounds **8**-**13** do not act as substrates. The only exception is **7** (R = H), which also should allow O_2 to bind to the heme iron because it is smaller than L-NIO and should be able to rotate, but **7** does not act as a substrate or as an inactivator. Although the hydrogen of the formamidino group of **7** can presumably rotate toward the heme, unlike L-NIO, whose methyl group can fill the void left by the rotated imino group, the hydrogen of **7** cannot, and the protonated imino group of **7** is not aligned properly to protonate the heme peroxide. Therefore, **7** does not act as a substrate or inactivator, as observed.

Compounds **8**, **9**, and **11** exhibit weak irreversible inhibition of iNOS at much higher concentrations than L-NIO (**4**); although the K_I increases with increasing size, the k_{inact} also increases, but the overall efficiency (k_{inact}/K_I) diminishes with size, and that for L-NIO is 17-61 times greater than the other three compounds. No inactivation was observed if the R group of the amidine was branched at the α-carbon atom, replacing one or both of the α-

protons, as in **10** and **12**. Compound **13** (R = Bn) also has a secondary carbon at that position but it is not an irreversible inhibitor, probably because its binding is so weak (K_i 2.4 mM).

Fast et al. reported that L-NIO is both an inactivator and a substrate of iNOS;[23] incubation of iNOS with L-NIO gives N^{ω}-hydroxy-L-NIO, which inactivates iNOS, although it is not on the inactivation pathway from L-NIO. Compound **22** was designed as the potential hydroxylation product of **8**, but no **22** was observed, again supporting the lack of detection of nitric oxide from incubation of **8** with iNOS. Furthermore, **22** did not inactivate iNOS.

Compound **8** is a time-, concentration-, and NADPH-dependent inhibitor of iNOS. To determine if inactivation proceeds by hydrogen atom abstraction from the amidino ethyl group, (*S*)-2-amino-5-(propanimidamido-2,2,3,3,3-d_5)pentanoic acid (**26**) was synthesized. Although it inactivated iNOS, it did so with no kinetic deuterium isotope effect on k_{inact} or k_{inact}/K_I (Table 3), consistent with an inactivation mechanism that does not involve amidine modification.

One other possible inactivation mechanism was tested: iNOS dimer disruption. The results, demonstrated by low temperature PAGE in the presence of H_4B and L-arginine (Figure 2 and Table 4), indicated that of the 65% SDS-resistant iNOS dimer that appeared in the control, only 16-19% was converted to iNOS monomer after inactivation with compounds L-NIO, **8**, **9**, and **11**. However, this does not account for complete loss of enzyme activity, although it could be one of the mechanisms of inactivation.

L-NIO[25] and 1400W[26] appear to inactivate iNOS by conversion of their heme cofactor to biliverdin, which requires molecular oxygen. With **8**, **9**, and **11**, which our computer model suggests prohibit oxygen binding, no biliverdin could be detected by HPLC with either UV or MS detection. Also, <5% of heme was lost by incubation of iNOS with **8**, **9**, or **11**. Therefore, the mechanism of inactivation of iNOS by these compounds cannot yet be determined but is definitely different from that by L-NIO,[25] where substrate turnover via *N*-hydroxylation; and methyl amidines L-NIO[25] and 1400W,[26] in which subsequent heme degradation were previously described.

CONCLUSIONS

A series of L-NIO analogues was synthesized to determine if the dual substrate/inactivation properties of L-NIO occurred throughout the series and if the size of the alkyl group determined the ratio of turnover to inactivation, as was observed for L-NIO[25] and 1400W[26]. None of the analogues acted as substrates for iNOS. All were inhibitors, with inhibitory activity diminishing with increased size of the amidine substituent, but only analogues **8** (R = Et), **9** (R = *n*-Pr), and **11** (R = *i*-Bu) produced irreversible inhibition. Although **7** (R = H) was the most potent inhibitor, even more potent than L-NIO, it did not inactivate iNOS. One common feature of the compounds that produced irreversible inhibition was the primary or secondary carbon adjacent to the imino carbon of the amidine group. Some iNOS dimer was lost (16-19%) with inactivation by **8**, **9**, and **11**, but that was not much different from the amount that was lost by L-NIO inactivation. However, unlike L-NIO, no nitric oxide was formed, no *N*-hydroxylated product was formed, no heme was lost, and no biliverdin was

formed upon inactivation of iNOS by **8**, **9**, and **11**. Therefore, the mechanism of inactivation of iNOS by **8**, **9**, and **11** is different from that with L-NIO and 1400W, but that mechanism is still unknown.

Supplementary Material

Refer to Web version on PubMed Central for supplementary material.

Acknowledgments

Funding

The authors are grateful for financial support from the National Institutes of Health (GM049725 to R.B.S. and GM057353 to T.L.P.).

REFERENCES

1. Kerwin JF, Heller M. The arginine-nitric oxide pathway: a target for new drugs. Med. Res. Rev. 1994; 14:23–74. [PubMed: 7508539]
2. Nakamura T, Lipton SA. Emerging roles of *S*-nitrosylation in protein misfolding and neurodegenerative diseases. Antioxid. Redox Signal. 2008; 10:87–101. [PubMed: 17961071]
3. Dawson VL, Dawson TM. Nitric oxide in neurodegeneration. Prog. Brain Res. 1998; 118:215–229. [PubMed: 9932444]
4. Vallance PP, Leiper JJ. Blocking NO synthesis: how, where and why? Nat. Rev. Drug Discov. 2002; 1:939–950. [PubMed: 12461516]
5. Calabrese V, Mancuso C, Calvani M, Rizzarelli E, Butterfield DA, Stella AMG. Nitric oxide in the CNS: Neuroprotection versus neurotoxicity. Nat. Neurosci. 2007; 8:766–775.
6. Hobbs AJ, Higgs A, Moncada S. Inhibition of nitric oxide synthase as a potential therapeutic target. Annu. Rev. Pharmacol. Toxicol. 1999; 39:191–220. [PubMed: 10331082]
7. Kerwin JF, Lancaster JR, Feldman PL. Nitric oxide: A new paradigm for secnd messengers. J. Med. Chem. 1995; 38:4343–4362. [PubMed: 7473563]
8. Ji H, Stanton BZ, Igarashi J, Li H, Martásek P, Roman LJ, Poulos TL, Silverman RB. Minimal pharmacophoric elements and fragment hopping, an approach directed at molecular diversity and isozyme selectivity. Design of selective neuronal nitric oxide synthase inhibitors. J. Am. Chem. Soc. 2008; 130(12):3900–3914. [PubMed: 18321097]
9. Steinert JR, Chernova T, Forsythe ID. Nitric oxide in brain function, dysfunction and dementia. The Neuroscientist. 2010; 16:435–452. [PubMed: 20817920]
10. Daff S. Nitric oxide synthase: Structures and mechanisms. Nitric Oxide: Biology and Chemistry. 2010; 23:1–11.
11. Crane BR, Arval AS, Ghosh DK, Wu C, Getzoff ED, Stuehr DJ, Tainer JA. Structure of nitric oxide synthase oxygenase dimer with pterin and substrate. Science. 1998; 279:2121–2126. [PubMed: 9516116]
12. Alderton WK, Cooper CE, Knowles RG. Nitric oxide synthases: Structure, function, and inhibition. Biochem. J. 2001; 357:593–615. [PubMed: 11463332]
13. Lambert LE, French JF, Whitten JP, Baron BM, McDonald IA. Characterization of cell selectivity of two novel inhibitors of nitric oxide synthesis. Eur. J. Pharmacol. 1992; 216:131–134. [PubMed: 1382020]
14. Adak S, Sharma M, Meade AL, Stuehr DJ. A conserved flavin-shielding residue regulates NO synthase electron transfer and nicotinamide coenzyme specificity. Proc. Natl. Acad. Sci. USA. 2002; 99:13516–13521. [PubMed: 12359874]
15. Siddhanta U, Presta A, Fan BC, Wolan D, Rousseau DL, Stuehr DJ. Domain swapping in inducible nitric-oxide synthase - electron transfer occurs between flavin and heme groups located on adjacent subunits in the dimer. J. Biol. Chem. 1998; 273:18950–18958. [PubMed: 9668073]

16. Hurshman AR, Krebs C, Edmondson DE, Huynh BH, Marletta MA. Formation of a pterin radical in the reaction of the heme domain of inducible nitric oxide synthase with oxygen. Biochemistry. 1999; 38:15689–15696. [PubMed: 10625434]
17. Wei C-C, Wang Z-Q, Wang Q, Meade AL, Hemann C, Hille R, Stuehr DJ. Rapid kinetic studies link tetrahydrobiopterin radical formation to heme-dioxy reduction and arginine hydroxylation in inducible nitric oxide synthase. J. Biol. Chem. 2001; 276:315–219. [PubMed: 11020389]
18. Wei C-C, Crane BR, Stuehr DJ. Tetrahydrobiopterin radical enzymology. Chem. Rev. 2003; 103:2365–2384. [PubMed: 12797834]
19. Stuehr DJ, Wei C-C, Wang ZQ, Hille R. Exploring the redox reactions between heme and tetrahydrobiopterin in the nitric oxide synthases. Dalton Trans. 2005; 21:3427–3435. [PubMed: 16234921]
20. Stuehr DJ, Wei CC, Santolini J, Wang Z-Q, Aoyagi M, Getzoff ED. Radical Reactions of Nitric Oxide Synthases. Biochem Soc. Symp. 2004; 71:39–49. [PubMed: 15777011]
21. Woodward JJ, NejatyJahromy Y, Britt RD, Marletta MA. Pterin- centered radical as a mechanistic probe of the second step of nitric oxide synthase. J. Am. Chem. Soc. 2010; 132:5105–5113. [PubMed: 20307068]
22. Wei C-C, Wang Z-Q, Tejero J, Yang Y-P, Hemann C, Hille R, Stuehr DJ. Catalytic reduction of a tetrahydrobiopterin radical within nitric oxide synthase. J. Biol. Chem. 2008; 283:11734–11742. [PubMed: 18283102]
23. Abu-Soud HM, Yoho LL, Stuehr DJ. Calmodulin controls neuronal nitric oxide synthase by a dual mechanism. Activation of intra- and interdomain electron transfer. J. Biol. Chem. 1994; 269:32047–32050. [PubMed: 7528206]
24. Sheta EA, McMillan K, Siler-Masters BS. Evidence for a bidomain structure of constitutive cerebellar nitric oxide synthase. J. Biol. Chem. 1994; 169:15147–15153. [PubMed: 7515050]
25. Fast W, Nikolic D, Van Breemen RB, Silverman RB, Mechanistic studies of the inactivation of inducible nitric oxide synthase by N^5-(1-iminoethyl)L-ornithine (l-NIO). J. Am. Chem. Soc. 1999; 121:903–916.
26. Zhu Y, Nikolic D, Silverman RB, Mechanism of Inactivation of Inducible Nitric Oxide Synthase by Amidines. Irreversible Enzyme Inactivation without Inactivator Modification. J. Am. Chem. Soc. 2005; 127:858–868. [PubMed: 15656623]
27. Böger RH, Bode-Böger SM. Asymmetric dimethylarginine, derangements of the endothelial nitric oxide synthase pathway, and cardiovascular diseases. Seminar Thromb. Homeostasis. 2000; 26:539–545.
28. Stuehr DJ, Ikeda-Saito M. Spectral characterization of brain and macrophage nitric oxide synthases. Cytochrome P-450-like hemeproteins that contain a flavin semiquinone radical. J. Biol. Chem. 1992; 267:20547–20550. [PubMed: 1383204]
29. Cheng Y-C, Prusoff WH. Relationship between the inhibition constant (K_I) and the concentration of inhibitor which causes 50 per cent inhibition (IC_{50}) of an enzymatic reaction. Biochem. Pharmacol. 1973; 22:3099–3108. [PubMed: 4202581]
30. Kitz R, Wilson IB. Esters of Methanesulfonic Acid as Irreversible Inhibitors of Acetylcholinesterase. J. Biol. Chem. 1962; 237:3245–3249. [PubMed: 14033211]
31. Case DA, Cheatham TE, Darden T, Gohlke H, Luo R, Merz KM, Onufriev A, Simmerling C, Wang B, Woods RJ. The Amber biomolecular simulation programs. J. Comp. Chem. 2005; 26:1668–1688. [PubMed: 16200636]
32. Shahrokh K, Orendt A, Yost GS, Cheatham TE 3rd. Quantum mechanically derived AMBER-compatible heme parameters for various states of the cytochrome P450 catalytic cycle. J Comput Chem. 2012; 33:119–133. [PubMed: 21997754]
33. Wang J, Wolf RM, Caldwell JW, Kollman PA, Case D. Development and testing of a general Amber force field. J. Amer. Chem. Soc. 2004; 25:1157–1174.
34. Jakalian A, Bush BL, Jack DB, Bayly CI. Fast, efficient generation of high-quality atom charges. AM1-BCC model: I. Method. J. Comp. Chem. 2000; 21:132–146.
35. Jakalian A, Jack DB, Bayly CI. Fast, efficient generation of high-quality atom charges. AM1-BCC model: II. Parameterization and validation. J. Comp. Chem. 2002; 23:1623–1641. [PubMed: 12395429]

36. Darden T, York D, Pedersen L. Particle mesh Ewald-an Nlog(N) method for Ewald sums in large systems. J. Chem. Phys. 1993; 103:8577–8593.
37. Miyamoto S, Kollman PA. SETTLE: An analytical version of the SHAKE and RATTLE algorithm for rigid water molecules. J. Comput. Chem. 1992; 13:952–962.
38. Litzinger EA, Martasek P, Roman LJ, Silverman RB. Design, synthesis, and biological testing of potential heme-coordinating nitric oxide synthase inhibitors. Bioorg. Med. Chem. 2006; 14:3185–3198. [PubMed: 16431112]
39. Moore WM, Webber RK, Jerome GM, Tjoeng FS, Misko TP, Currie MG. l-N^6-(1-Iminoethyl)lysine: A selective inhibitor of inducible nitric Ooxide synthase. J. Med. Chem. 1994; 37:3886–3888. [PubMed: 7525961]
40. Hah J, Roman LJ, Martasek P, Silverman RB, Reduced amide bond peptidomimetics. (4*S*)-*N*-(4-Amino-5-[aminoalkyl]aminopentyl)-*N*‘-nitroguanidines, potent and highly selective inhibitors of neuronal nitric oxide synthase. J. Med. Chem. 2001; 44:2667–2670. [PubMed: 11472219]
41. Li D, Shi F, Deng Y. One-step C=N, C=O bonds cleavage and C=O, C=N bonds formation over supported ionic liquid in water. Tetrahedron Lett. 2004; 45:6791–6794.
42. Segel, IH. Enzyme Kinetics. John Wiley & Sons; New York: 1975. p. 105
43. Hevel JM, Marletta MA. Nitric oxide synthase assays. Meth. Enzymol. 1994; 233:250–258. [PubMed: 7516999]
44. Huang H, Hah J, Silverman RB. Mechanism of nitric oxide synthase. Evidence that direct hydrogen atom abstraction from the O−H bond of N^G-hydroxyarginine is not relevant to the mechanism. J. Am. Chem. Soc. 2001; 123:2674–2676. [PubMed: 11456942]
45. Aswad DW. Determination of d- and l-aspartate in amino acid mixtures by high- performance liquid chromatography after derivatization with a chiral adduct of *o*-phthaldialdehyde. Anal. Biochem. 1984; 137:405–409. [PubMed: 6731824]
46. Klatt P, Schmidt K, Lehner D, Glatter O, Bächinger HP, Mayer B. Structural analysis of porcine brain nitric oxide synthase reveals a role for tetrahydrobiopterin and l-arginine in the formation of an SDS-resistant dimer. EMBO J. 1995; 14:3687. [PubMed: 7543842]
47. Fedorov R, Ghosh DK, Schlichting I. Crystal structures of cyanide complexes of P450cam and the oxygenase domain of inducible nitric oxide synthase-structural models of the short-lived oxygen complexes. Arch. Biochem. Biophys. 2003; 409:25–31. [PubMed: 12464241]
48. Li H, Roman CS, Martásek P, Masters BSS, Poulos TL. Crystallographic Studies on Endothelial Nitric Oxide Synthase Complexed with Nitric Oxide and Mechanism-Based Inhibitors. Biochemistry. 2001; 40:5399. [PubMed: 11331003]

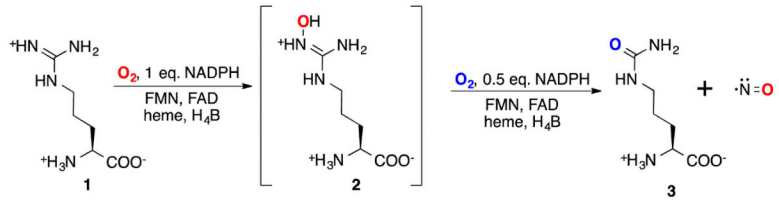

Scheme 1.

Nitric oxide synthase-catalyzed conversion of L-arginine (**1**) to L-citrulline (**3**) and NO

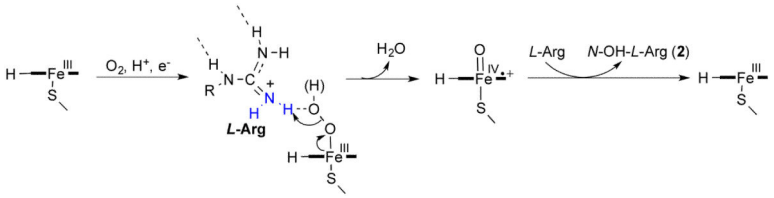

Scheme 2.

General mechanism for the first step of the NOS reaction

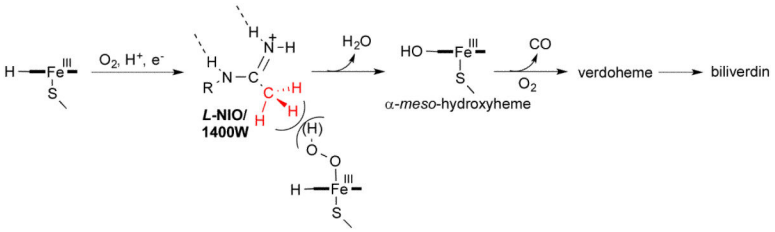

Scheme 3.

The proposed mechanism of L-NIO and 1400W inactivation with iNOS.[26]

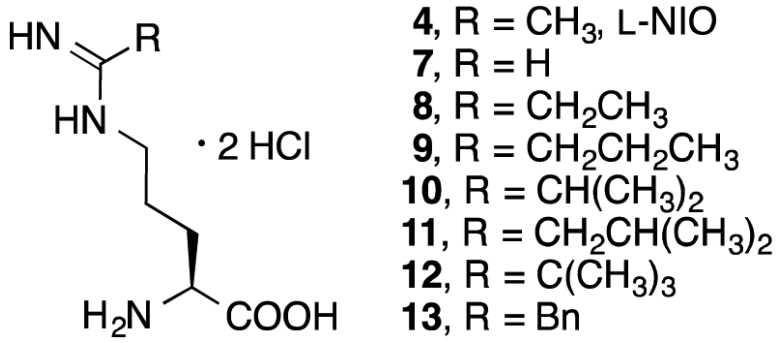

Figure 1.
Analogues of L-NIO

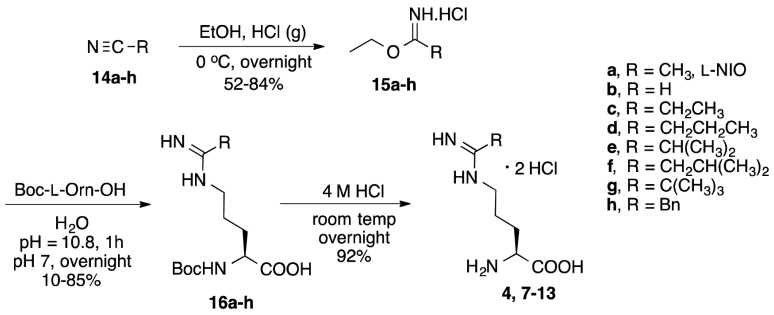

Scheme 4.

Synthesis of compounds **4, 7-13**

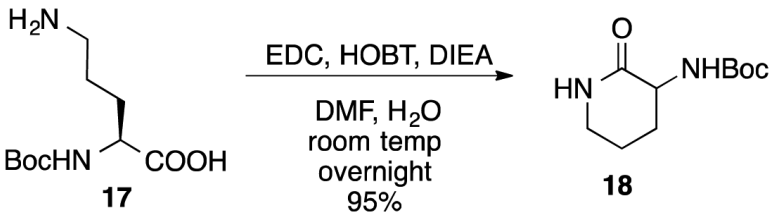

Scheme 5.

Method to remove **17** from the reaction mixture

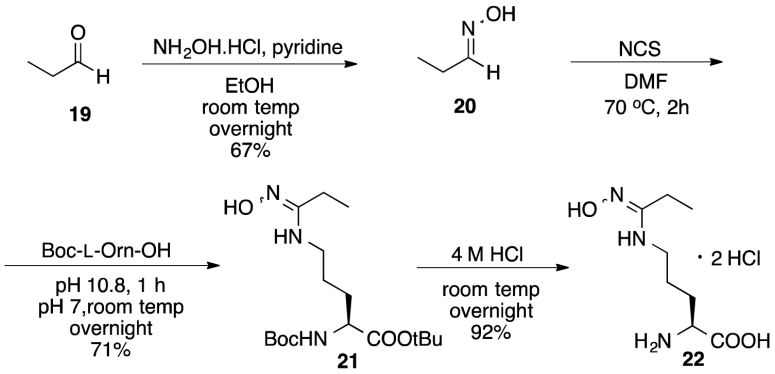

Scheme 6.

Synthesis of compound **22**

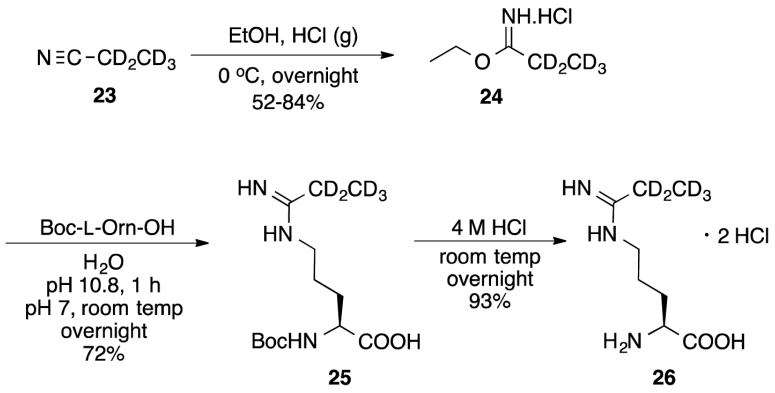

Scheme 7.
Synthesis of **26**

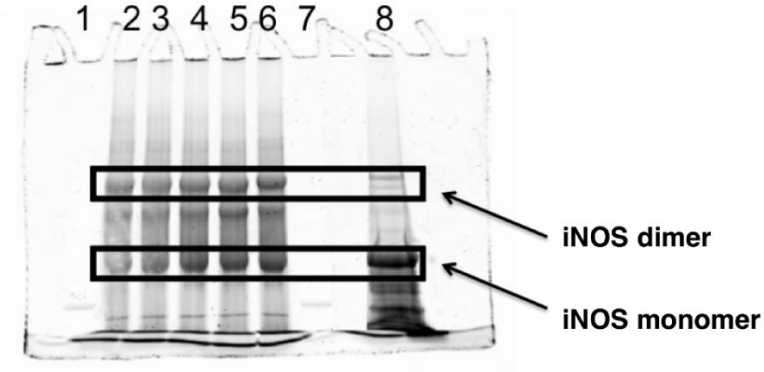

Figure 2.

LT-PAGE gel of iNOS with L-NIO (**4**), **8**, **9**, and **11**. Lane 2, native iNOS; lane 3, **4**; lane 4, **8**; lane 5, **9**; lane 6, **11**, lane 8, denatured iNOS

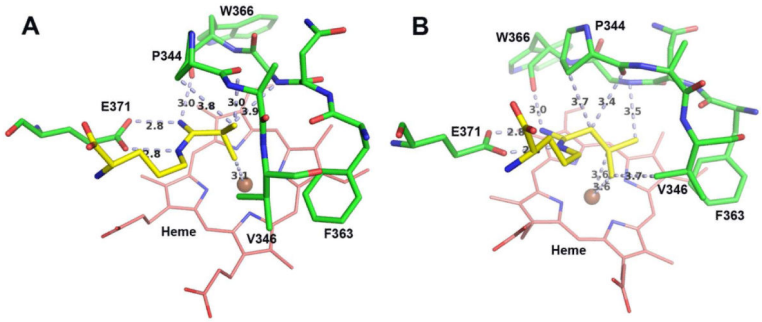

Figure 3.

Models of (**A**) **10** and (**B**) **11** right after the initial minimization. Major distances less than 4.0 Å are marked in Å including the three H-bonds that anchor the inhibitor to the NOS active site glutamate. The figure was prepared with PyMol (www.pymol.org).

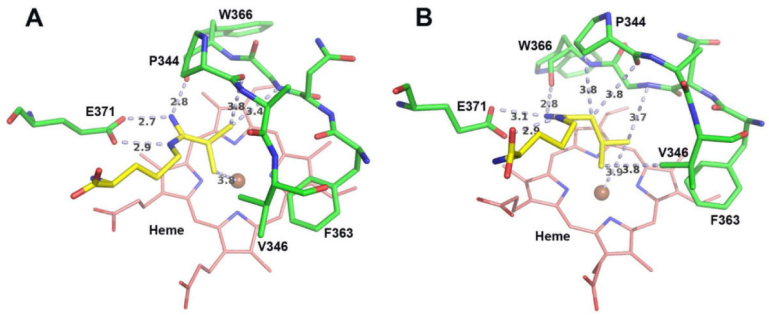

Figure 4.

Models of (**A**) **10** and (**B**) **11** in the final frame of the simulation. Major distances less than 4.0 Å are marked in Å including the three H-bonds that anchor the inhibitor to the NOS active site glutamate. The figure was prepared with PyMol (www.pymol.org).

Table 1

IC_{50} and K_i values for compounds **4, 7-13** against iNOS

Compound	IC_{50}(μM)[a]	K_i(μM)[b]
4 (L-NIO)	8.1	3.65
7	0.4	0.18
8	16.1	7.25
9	19.1	8.61
10	138	65.18
11	68.7	30.95
12	323	146
13	5333	2402

[a]The apparent IC_{50} values are represented as the mean from two or more independent experiments performed in duplicate with five or six data points each and correlation coefficients of 0.92-0.99. The experimental standard deviations were less than 10%.

[b]The apparent K_i values were obtained by measuring the percent enzyme inhibition in the presence of 10 μM L-arginine with at least five concentrations of inhibitor. The parameters of the following inhibition equation[42] were fitted to the initial velocity data: % inhibition = $100[I]/([I]+K_i(1+[S]/K_m))$. K_m value for L-arginine was 8.2 μM (iNOS).

Table 2

Kinetic constants for **4, 8, 9**, and **11**

	L-NIO (4)	8	9	11
k_{inact}(min^{-1})	0.073 ± 0.003	0.0743 ± 0.0073	0.131 ± 0.0095	0.347 ± 0.006
K_I(μM)	13.7 ± 1.6	243 ± 31.4	674 ± 80	4009 ± 426
k_{inact}/K_I ($\mu M^{-1}.min^{-1}$)	0.0053 ± 0.0007	0.00031 ± 0.000028	0.00020 ± 0.0000096	0.000087 ± 0.000011

Table 3

Kinetic Isotope Effect on iNOS inactivation by **8** and **26**

	8	**26**	**H/D**
k_{inact}(min^{-1})	0.0743 ± 0.0073	0.073 ± 0.0063	1.025 ± 0.071
K_I(μM)	243 ± 31.4	278 ± 27.7	0.884 ± 0.068
k_{inact}/K_I ($\mu M^{-1}.min^{-1}$)	0.00031 ± 0.000028	0.000265 ± 0.000015	1.159 ± 0.108

Table 4

Amount of dimer remaining after inactivation

Lane		% iNOS Dimer
2	Native iNOS	65 ± 5
3	**4** with iNOS	51 ± 4
4	**8** with iNOS	46 ± 2
5	**9** with iNOS	47 ± 5
6	**11** with iNOS	49 ± 5
8	Denatured iNOS	<2